Published April , 2010

Energetics of gating at the apo–acetylcholine receptor transmitter binding site

Prasad Purohit and Anthony Auerbach

Department of Physiology and Biophysics, State University of New York at Buffalo, Buffalo, NY 14214

Acetylcholine receptor channels switch between conformations that have a low versus high affinity for the transmitter and conductance for ions (R↔R*; gating). The forward isomerization, which begins at the transmitter binding sites and propagates ∼50 Å to the narrow region of the pore, occurs by approximately the same sequence of molecular events with or without agonists present at the binding sites. To pinpoint the forces that govern the R versus R* agonist affinity ratio, we measured single-channel activation parameters for apo-receptors having combinations of mutations of 10 transmitter binding site residues in the α (Y93, G147, W149, G153, Y190, C192, and Y198), ε (W55 and P121), or δ (W57) subunit. Gating energy changes were largest for the tryptophan residues. The αW149 energy changes were coupled with those of the other aromatic amino acids. Mutating the aromatic residues to Phe reduces the R/R* equilibrium dissociation constant ratio, with αY190 and αW149 being the most sensitive positions. Most of the mutations eliminated long-lived spontaneous openings. The results provide a foundation for understanding how ligands trigger protein conformational change.

INTRODUCTION

The neuromuscular acetylcholine (ACh) receptor (AChR) is an allosteric protein in which a change in affinity for ACh at two transmitter binding sites is coupled with a global gating conformational change that regulates ionic conductance (Edelstein and Changeux, 1998; Karlin, 2002; Lester et al., 2004; Sine and Engel, 2006; Auerbach, 2010). In the absence of agonists, wild-type (wt) AChRs rarely switch from the nonconducting R shape to the ion-conducting R* shape, but, after binding two transmitter molecules, the probability of this occuring increases dramatically.

The magnitude of the diliganded gating equilibrium constant (E_2) is the product of two fundamental parameters: the intrinsic tendency of the protein to isomerize spontaneously (the unliganded gating equilibrium constant, E_0) and the change in affinity for agonists at each of the two transmitter binding sites (the R/R* equilibrium dissociation constant ratio, K_d/J_d; Fig. 1). In adult mouse wt neuromuscular AChRs activated by ACh (−100 mV at 23°C), E_2 = ∼28 (Chakrapani et al., 2003), which is the product of E_0 (= $\sim 6.5 \times 10^{-7}$) times $(K_d/J_d)^2$ (= ∼6,600)^2 (Jha and Auerbach, 2010). From the natural logarithm of (K_d/J_d), we estimate that each of the two ACh molecules is more stably bound to R* versus R by ∼5.2 kcal/mol.

It is of interest to pinpoint and characterize the molecular forces that underlie the difference in ACh binding energy, R versus R*. Each AChR transmitter binding site has five aromatic residues that are important to both ligand binding and channel gating (Fig. 2). With ACh as the agonist, point mutations of these positions increase K_d and decrease E_2 (Aylwin and White, 1994; O'Leary et al., 1994; Sine et al., 1994; Chen et al., 1995; Akk et al., 1996, 1999; Chiara et al., 1998; Akk, 2001; Bafna et al., 2009). It has been difficult to probe in detail the role of these aromatic residues because their mutation can reduce the affinity for agonists to such a degree that measuring currents from diliganded AChRs becomes impossible. As a consequence, the extent to which mutations of these residues change E_0 versus K_d/J_d is unknown. It is possible, however, to quantify the gating energy changes experienced by these residues in mutant AChRs that spontaneously undergo the R↔R* isomerization in the absence of exogenous ligands (Purohit and Auerbach, 2009). Probing the binding site residues in apo-AChRs not only reveals their energy contributions to binding and gating but is also likely to reflect their behaviors in the presence of agonists because the mechanism of gating is approximately the same with and without ligands (Purohit and Auerbach, 2009). In this study, we estimate E_0 for 123 different mutations of 10 different amino acids at the adult mouse neuromuscular AChR transmitter binding sites.

MATERIALS AND METHODS

Mutants were made by using the QuikChange Site-Directed Mutagenesis kit (Agilent Technologies) and were confirmed by complete cDNA sequencing. Human embryonic kidney 293 cells were

Correspondence to Anthony Auerbach: auerbach@buffalo.edu

Abbreviations used in this paper: ACh, acetylcholine; AChBP, ACh-binding protein; AChR, ACh receptor; wt, wild type.

The Rockefeller University Press $30.00
J. Gen. Physiol. Vol. 135 No. 4 321–331
www.jgp.org/cgi/doi/10.1085/jgp.200910384

Supplemental Material can be found at:
http://jgp.rupress.org/content/suppl/2010/03/22/jgp.200910384.DC1.html

Published April , 2010

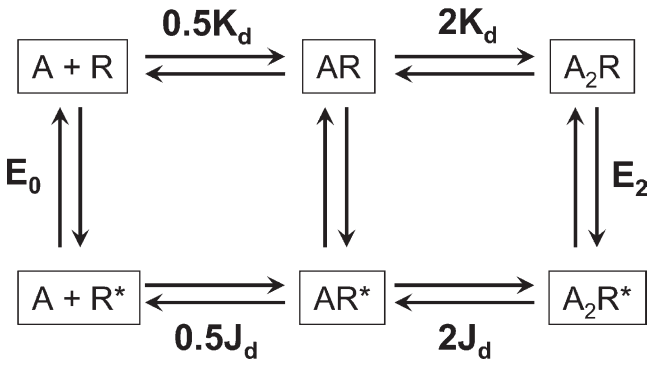

Figure 1. Cyclic scheme for AChR activation. Stable conformations are boxed, equilibrium constants are bold, and transient intermediate states are represented by arrows. R, conformation with a low affinity for agonists and a nonconducting channel; R*, conformation with a high affinity for agonists and a conducting channel; A, the agonist. The two binding sites are equivalent. K_d and J_d are the equilibrium dissociation constants from R and R*. E_0 and E_2 are the gating equilibrium constants for the apo- and diliganded protein. The energy difference between any two stable states is independent of the connecting pathway, so $E_2/K_d^2 = E_0/J_d^2$ or $E_2 = E_0(K_d/J_d)^2$.

transiently transfected using calcium phosphate precipitation with a mixture of cDNAs encoding mouse muscle AChRs (α, β, δ, and ε; ∼3–4 μg/35-mm dish in a 2:1:1:1 ratio). 0.1 μg/μl cDNA encoding green fluorescent protein was added as a marker to the transfection cocktail. The cells were incubated at 37°C; the culture medium was washed after ∼16 h, and single-channel patch clamp recording was performed in the cell-attached configuration (Hamill et al., 1981) ∼4–6 h later at 23°C. Currents were sampled at 50 kHz after low-pass filtering at 20 kHz. QuB software (State University of New York at Buffalo) was used to acquire and analyze the single-channel currents.

The bath solution was Dulbecco's phosphate-buffered saline containing 137 mM NaCl, 0.9 mM $CaCl_2$, 2.7 mM KCl, 1.5 mM KH_2PO_4, 0.5 mM $MgCl_2$, and 8.1 mM Na_2HPO_4, pH 7.4. The pipette solution was the same as the bath, and the pipette potential was 70 mV, which corresponds to a membrane potential (V_m) of approximately −100 mV. The pipette solution contained no added agonist, and the pipette holder/electrodes were never exposed to an AChR agonist.

In wt AChRs, unliganded openings are both rare and brief. To increase both the frequency and duration of such openings, we used a background construct that had multiple point mutations in both α subunits: (αD97A+αY127F+αS269I [DYS]). Individually, each of these mutations increases the diliganded gating equilibrium constant (E_2; αD97A, 168-fold [Chakrapani et al., 2003]; αY127F, 59-fold [Purohit and Auerbach, 2007]; αS269I, 115-fold [Mitra et al., 2005]) by an approximately parallel change in the unliganded gating equilibrium constant (E_0; Purohit and Auerbach, 2009). None of the mutations had a measurable effect on K_d. If the energetic consequence of each mutation is independent of the others, we estimate that the net increase in E_0 in this background is $168 \times 59 \times 115 = 1.10^6$. The fold changes in E_0 of the binding site mutations in this study are expressed in reference to the DYS background, so the only assumption we make is that the binding site and DYS mutations (combined) have independent energetic consequences. Expression was robust for most mutant constructs. Because there was no ACh in the pipette solution, there was no agonist-associated open-channel block, and the single-channel current amplitude was in all cases ∼7 pA.

We define E_0 as the R↔R* isomerization equilibrium constant in the absence of exogenous agonist molecules and under the aforementioned experimental conditions. A mutation that changes E_0 changes the relative free energy difference between the R and R* shapes of the apo-AChR. This energy difference could be generated by altered interactions between any or all of the structural elements that comprise the apo-AChR transmitter binding site, including the protein, water molecules, and ions.

QuB software was used to acquire and analyze the single-channel currents. The raw data were corrected for baseline drift. Clusters of single-channel openings were then selected by eye, and the currents were idealized into noise-free conducting/nonconducting intervals by using a segmental k-means algorithm (Qin, 2004). To estimate unliganded opening (f_0) and closing (b_0) rate constants, the idealized current intervals were modeled using the maximum interval likelihood method after imposing a 25-μs dead time and missed event correction (Qin et al., 1997).

The fold change in E_0 (= f_0/b_0) for each mutant was estimated as E_0^{mutant}/E_0^{DYS}. The change in the free energy (ΔΔG) as a result of mutation was estimated as ΔΔG (kilocalories/mole) = −0.59 natural logarithm (ln; E_0^{mutant}/E_0^{DYS}). The coupling energy between side chains was calculated as ΔΔG (kilocalories/mole) = −0.59 ln (observed E_0^{mutant}/predicted E_0^{mutant}). The predicted value was calculated as the sum of the ΔΔG values for each individual mutation.

In almost all of the binding site mutants (94%; 104 of 111 constructs on the DYS background), the spontaneous open- and closed-interval durations were described by a single exponential component. For these, f_0 and b_0 were the inverse mean lifetime of the nonconducting and conducting intervals. For the remaining constructs (wt, αY93G, αY190G, αG153S, and ε/δW55/57 R and E), both brief (∼0.25 ms) and long (∼1.0 ms) open-interval components were apparent. For these constructs, interval durations were fitted by a kinetic model having two nonconducting and two conducting states. We tested both the COOC and OCCO kinetic schemes, with nearly equivalent results for the E_0 estimate. The values reported in the tables were obtained by using the first model, with E_0 calculated as the ratio of f_0/b_0 associated with the predominant (∼90%), brief component.

We define a range energy value as the natural logarithm of the ratio of the largest/smallest E_0 value for a series of mutations of one position (Jha et al., 2009). This parameter is a minimum estimate of the sensitivity of a position to perturbation in R↔R* gating. The interaction energy between residues was determined for a handful of side chain substitutions of each pair. The maximum observed interaction energy (the coupling range energy) is a minimum estimate of the extent to which side chains of the two positions can be coupled energetically. Additional mutations (both natural and unnatural) may increase the range energy and coupling range energy estimates. Φ is the unweighted, straight-line slope of the rate equilibrium (R/E) plot, which is f_0 versus E_0 on a log–log scale.

Online supplemental material

Figs. S1–S5 show example clusters and coupling energy estimates for transmitter binding site aromatic mutant pairs. The rate and equilibrium constants are given in Tables S1–S6. Online supplemental material is available at http://www.jgp.org/cgi/content/full/jgp.200910384/DC1.

RESULTS

The unliganded *Torpedo* AChR structure is shown in Fig. 2. The two transmitter binding sites are in the extracellular domain of the α subunit, close to the interface with the ε or δ subunit. Each binding site has

Published April , 2010

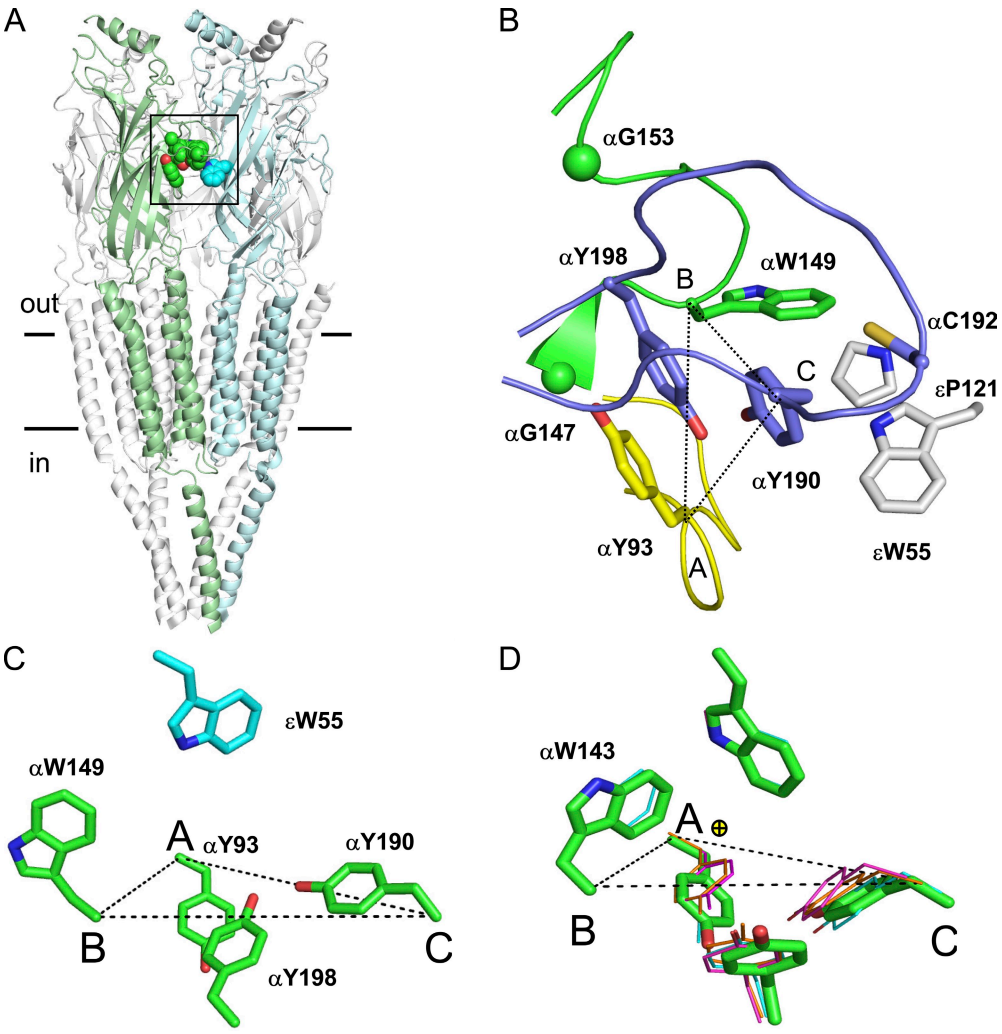

Figure 2. The AChR transmitter binding site. (A) Unliganded *Torpedo* AChR (2bg.pdb9; Unwin, 2005). α subunit, green; ε subunit, light blue. The binding site aromatic residues are shown as spheres (horizontal lines, membrane). (B) Close-up of the αε-transmitter binding site (boxed area in A) showing the salient residues in loop A (yellow), loop B (green), loop C (purple), and the ε subunit (gray; O, red; N, blue; S, yellow). αG147 and αG153 Cα atoms are spheres. Dotted lines connect Cα atoms from αY93 (loop A), αW149 (loop B), and αY190 (loop C). (C) In the AChR, αW149 and εW55 are spread. (D) In AChBP, the two tryptophans are edge to face in apo- and all liganded structures. No ligand, green (1UV6.pdb; Celie et al., 2004); nicotine, magenta (1UW6.pdb; Celie et al., 2004); carbamylcholine, orange (1UV6.pdb; Celie et al., 2004); and HEPES, cyan (1I9B.pdb; Brejc et al., 2001). Yellow sphere, quaternary amine of carbamylcholine.

several conserved aromatic side chains, namely Y93 (loop A), W149 (loop B), Y190 and Y198 (loop C) in the α subunit (the primary side of the binding site), and W57/55 in the adjacent δ/ε subunit (the complementary side; strand β_2). The nonaromatic binding site residues we investigated are αG147 and αG153 (loop B), αC192 (loop C), and εP121 (between strands β_6 and $\beta_{6'}$).

Point mutations of aromatic residues

Position αW149 was mutated to all 19 natural side chains (Fig. 3). These mutants were expressed on a high gain of function background construct (αD97A+αY127F+αS269I [DYS]). This combination of mutations increases the unliganded gating equilibrium constant E_0 about a million-fold but does not affect K_d for ACh, the K_d/J_d affinity ratio for ACh, or the gating conformational pathway. In this construct, spontaneous R↔R* gating intervals arising from individual apo-AChRs occur in clusters (Fig. 3 A, top; Purohit and Auerbach, 2009). We assumed that the fold changes in E_0 caused by the αW149 mutations on the DYS background are the same as would have occurred on the wt background.

We were unable to record single-channel currents from cells transfected with the αW149D or αW149E mutants either because of low expression in the cell membrane or because the probability of observing openings was extremely low. AChRs having 1 of the 17 remaining mutant side chains produced clustered openings from which we could estimate the single-channel, unliganded R→R* (f_0) and R←R* (b_0) rate constants and the corresponding reaction equilibrium constant ($E_0 = f_0/b_0$). Furthermore, because we know these values for the background construct alone, we can calculate the fold changes in f_0 and E_0 caused specifically by each αW149 side chain substitution (Table S1). AChRs with wt transmitter binding sites that are active spontaneously show both brief and long components in the open-interval duration histograms (Jackson, 1984, 1986; Grosman and Auerbach, 2000; Grosman, 2003; Purohit and Auerbach, 2009). All 17 of the αW149 mutations completely eliminated the long open component (Fig. 3 B).

Published April , 2010

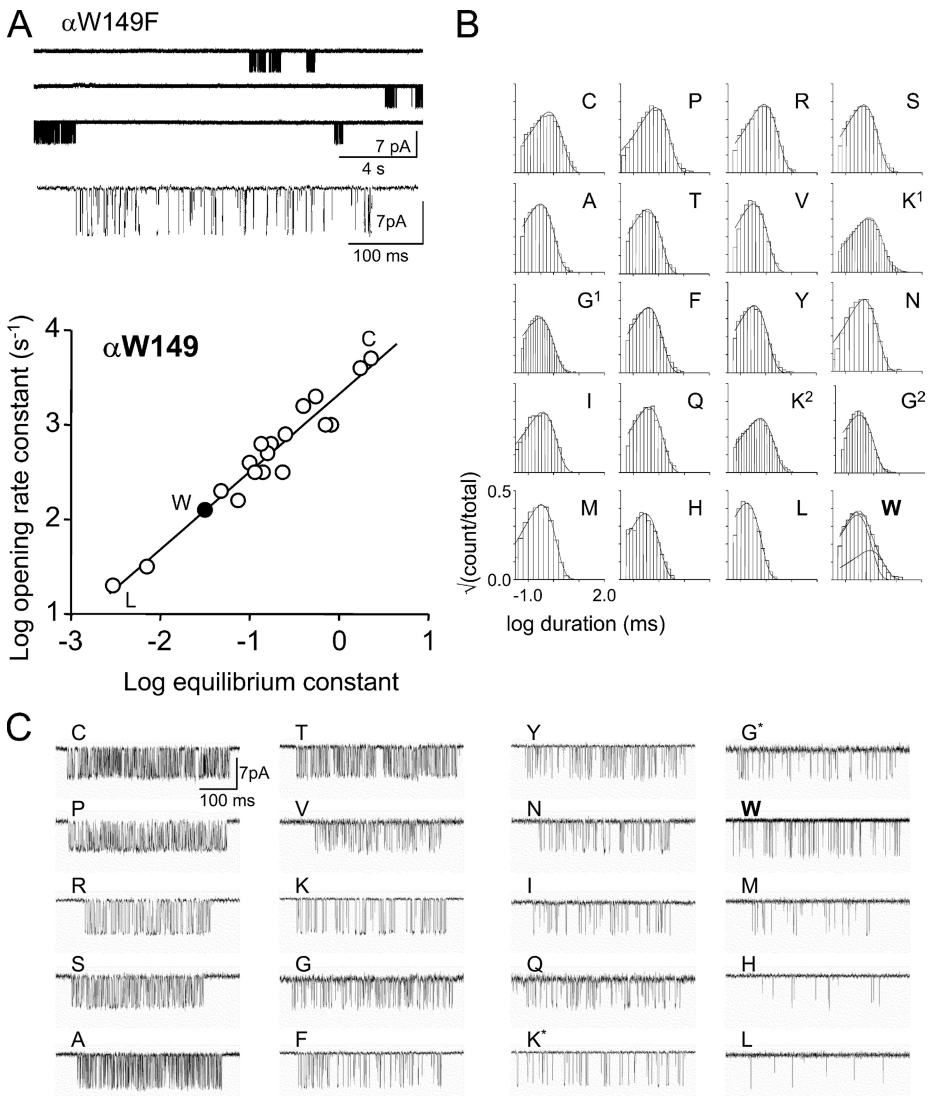

Figure 3. Mutations of αW149. (A) Spontaneous currents from αW149F (conducting is down; DYS background). (top) Long gaps between clusters are epochs when all of the AChRs in the patch are in states associated with desensitization. (middle) A cluster at higher resolution. The closed and open intervals reflect unliganded R↔R* gating. (bottom) Rate equilibrium (R/E) plot for αW149. Solid circle, wt. Most mutations increased the spontaneous gating equilibrium constant (E_0) relative to the wt. The ratio of the largest (Cys) to smallest (Leu) E_0 value represents an energy difference of 4.0 kcal/mol. (B) Open-interval duration histograms. All side chains except W have a single open-interval component. (C) Example of unliganded clusters from αW149 mutants (low-pass filtered to 2 kHz; Asp and Glu substitutions did not yield functional AChRs). Only the Gly and Lys mutations showed two distinct kinetic forms (marked by asterisks).

Most of the αW149 mutants increased E_0 and, thus, the probability of adopting R*. This indicates that AChRs bearing these side chains are more energetically stable in R* versus R compared with the wt. The three exceptions were Met, His, and Leu, which were modestly less stable in R*. Equilibrium constants are functions of the free energy difference between R and R*, and from our measurements we cannot determine the extent to which the changes in E_0 specifically arose from changes in the stability of either end state conformation.

We define the energy difference between the smallest and largest values of E_0 for a series of mutations of one position as the range energy, which is a minimum estimate of the energy sensitivity of that position in the R↔R* isomerization (Jha et al., 2009). The largest fold increase in E_0 at αW149 was with a Cys substitution (∼53-fold), and the largest fold decrease was with a Leu substitution (∼17-fold). Thus, an L to C substitution at position αW149 causes an ∼885-fold change in E_0, and the αW149 range energy (for both α subunits combined) is ∼4.0 kcal/mol.

The results for the αW149 mutants are summarized in the form of a rate equilibrium (R/E) plot in Fig. 3 A. The slope of this relationship, Φ, is a number between one and zero that reflects the relative timing (early to late) of the energy change experienced by the perturbed side chain between its structures in R versus R* (Auerbach, 2005; Zhou et al., 2005). The high Φ value for position αW149 (0.82 ± 0.04) suggests that its gating energy change occurs near the beginning of the forward isomerization process, about the same time as the energy change of the agonist molecule (Φ = ∼0.91; Grosman et al., 2000).

The effects of mutating the complementary binding site Trp residues εW55 and δW57 have been reported previously (Akk, 2002; Bafna et al., 2009). With regard to unliganded AChRs, the range energy for each of these two positions was 1.1 kcal/mol (W to H) and 1.7 kcal/mol (L to H), respectively (Bafna et al., 2009).

Published April , 2010

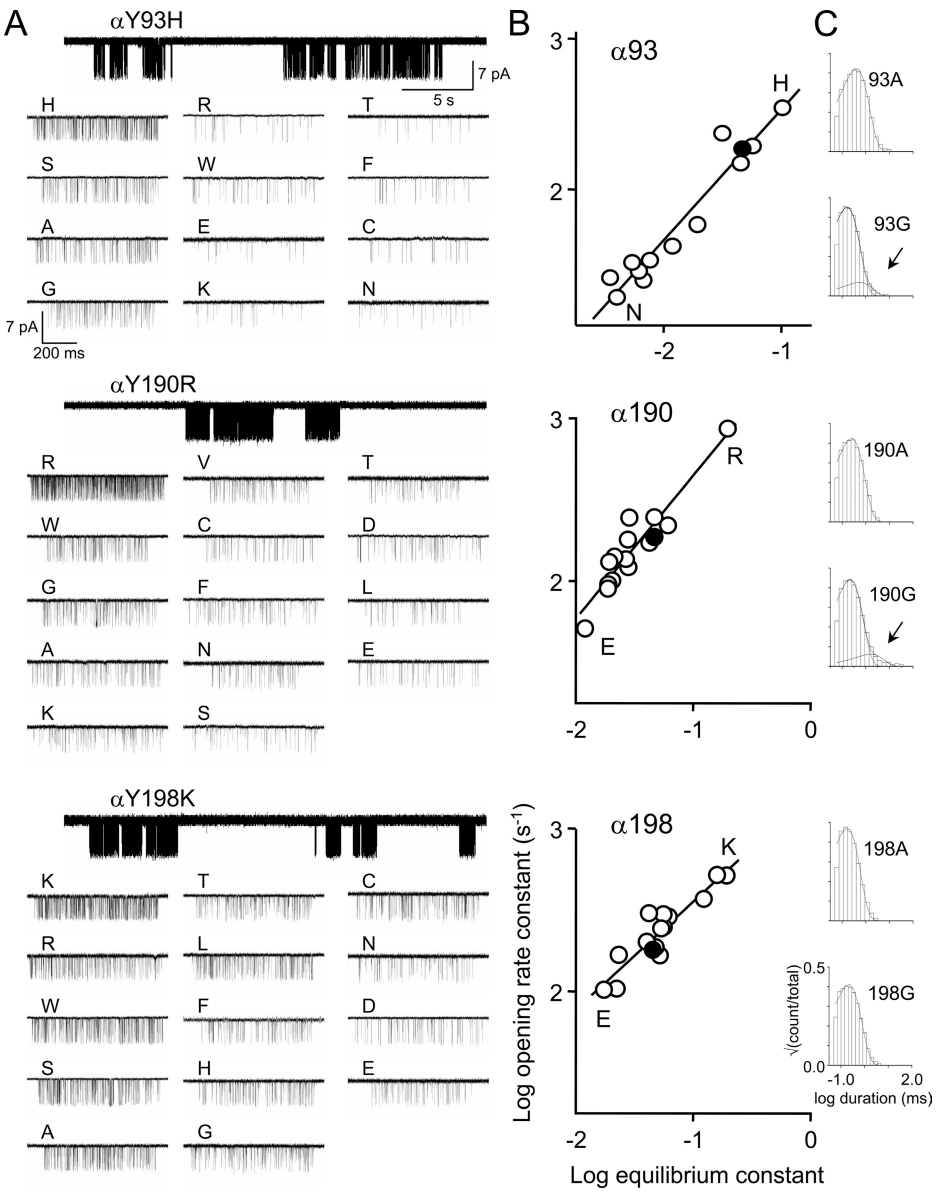

Figure 4. Mutations of αY93, αY190, and αY198. (A) Single-channel current traces at low (top) and high resolution. (B) Rate equilibrium plots. Filled circles, wt. αY93, αY190, and αY198 all exhibit smaller range energies (2.0 kcal/mol, 1.6 kcal/mol, and 1.4 kcal/mol, respectively) compared with αW149 (4.0 kcal/mol; Fig. 3 A). (C) Example of open-interval duration histograms. All construct mutants had a single open-interval component except αY93G and αY190G. Arrows indicate longer open components.

To compare these energies with those from the α-subunit side (for which there are two mutations per AChR), we estimated the degree of energy coupling between εW55 and δW57. The sums of the energy changes for the Glu or Arg individual mutations of the two complementary tryptophans were similar to those observed in the double mutants, indicating that the energetic consequences of the mutations are approximately independent (Fig. S5 and Table S4). We estimate that the range energy for εW55 and δW57 combined (εH+δH to εW+δL) is ∼2.8 kcal/mol.

We performed similar analyses of unliganded gating for mutations of the three tyrosine residues αY93, αY190, and αY198 (Fig. 4 and Table S2). At these positions, Asp and Glu substitutions produced functional AChRs that had a reduced E_0, except for the αY93D construct, for which no currents were observed. The range energy values for these three positions were 2.0 kcal/mol, 1.6 kcal/mol, and 1.4 kcal/mol, respectively, all smaller than for each of the two tryptophan positions. The slopes of the R/E plots for αY93, αY190, and αY198 were 0.86 ± 0.06, 0.88 ± 0.09, and 0.66 ± 0.06, respectively. In 95% (38 of 40) of the Tyr mutations, only a single spontaneous open time component was apparent. Histograms from the two exceptions, αY93G and αY190G, are shown in Fig. 4 C.

Pairwise mutations of aromatic residues

In the next set of experiments, we measured the extent to which the energy changes in the aromatic residues are independent of each other (Fig. 5, Figs. S1 and S2, and Tables S3 and S4; Horovitz and Fersht, 1990). First, αW149 was mutated in combination with side chain substitutions αY190, αY198, or αY93. Six different pairs

Published April , 2010

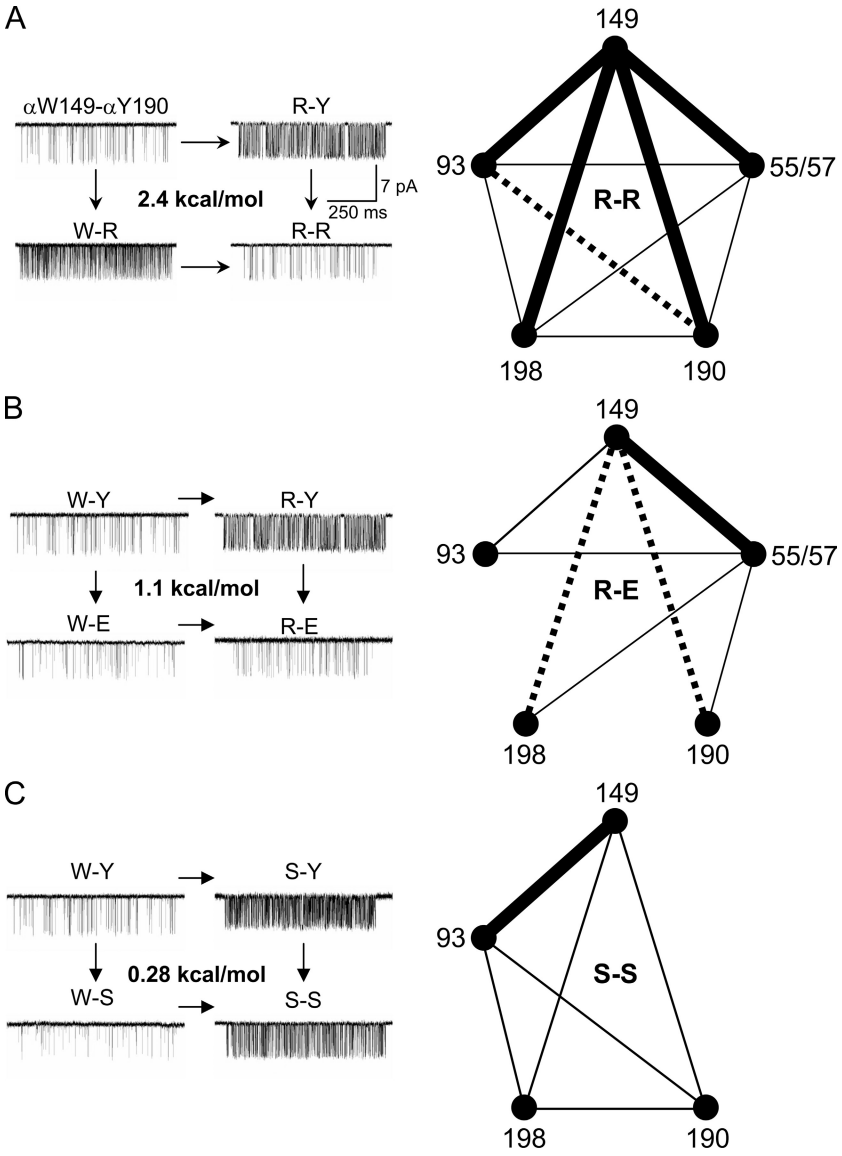

Figure 5. Energy coupling between aromatic residues. (A–C, left) Example of clusters for αW149–αY190 mutant pairs. (A–C, right) Coupling diagrams (thick lines, >2 kcal/mol; dashed lines, 1–2 kcal/mol; thin lines, <1 kcal/mol; no line, interaction not studied). (A) R–R substitutions. (left) An R mutation at α149 or α190 increases E_0, but both R mutations reduce E_0 (coupling energy, 2.4 kcal/mol). (right) With R substitutions, all aromatic residues are coupled to αW149 by >2 kcal/mol. (B) R–E substitutions. αW149 interactions are strongest with ε55(δ57) and nil with αY93. (C) S–S substitutions. The only strong interaction is between α149 and α93 (Figs. S1–S5 and Tables S3 and S4).

of side chains were probed to estimate the 149–190 interaction (coupling) energy (Y–W, S–S, A–A, R–D, R–E, and R–R). When both 149 and 190 were mutated to Arg, the observed E_0 was substantially smaller than predicted from independence (Fig. 5 A, left). This R–R combination exhibited 2.4 kcal/mol (unfavorable) interaction energy. When the side chains at these two positions were swapped (Y–W), or with the R–D or R–E pairs, the combined effect showed an intermediate, ∼1.1 kcal/mol deviation from independence (Fig. 5 B, left). When both residues were mutated to Ser or Ala (Fig. S1 A), the observed E_0 was very close to that predicted from independent action (Fig. 5 C, left).

The coupling patterns for 149–198 and 149–93 mutant pairs were similar, but not identical, to that for 149–190 (Table S3). The R–R substitutions for all three pairs showed a similarly high degree of coupling, ∼2.4 kcal/mol. The R–D pairs also were similarly coupled at 149–190 and 149–198 (1.1 kcal/mol). The A–A pairs showed no (149–198, −0.2 kcal/mol) or some (149–93, 0.8 kcal/mol) energetic coupling. The 149–93 R–E pair behaved approximately independently, whereas this combination at 149–198 and 149–190 showed some coupling (1.5 kcal/mol and 1.1 kcal/mol, respectively). Although S–S at 149–190 and 149–198 show little or no coupling, these two side chains interact strongly (2.4 kcal/mol) in the 149–93 pair. In summary, the interaction pattern was different for 149–93 compared with 149–190 and 149–198 for three different side chain pairs (S–S, A–A, and R–E). S–S and R–R pairwise interactions between the three tyrosines are shown in Fig. S2 and Table S3. In all cases, the interaction energy was intermediate (∼1.3 kcal/mol) for R–R combinations.

We also measured the coupling energy between the four α-subunit aromatic residues and the complementary δ/ε W57/55 (Figs. S3 and S4 and Table S4). The pairwise

Published April , 2010

interaction energies were mostly small (<1 kcal/mol). Larger interaction energies were apparent for the R–R pairs (∼2.2 kcal/mol) and for the R–E pair, which was more strongly coupled at the α–δ interface (2.1 kcal/mol) than at the α–ε interface (0.9 kcal/mol). The constructs εW55E+δW57E and εW55R+δW57R showed little coupling (<0.5 kcal/mol). However, αW149R+εW55E+δW57E showed a coupling energy of 1.4 kcal/mol. This suggests that with an R (but not a W) at position α149, the two complementary positions interact. The coupling energies for R–R, R–E, and S–S pairs are summarized in the diagrams in Fig. 5. AChRs having all four α-subunit aromatic positions mutated to R (in both subunits) expressed successfully (Fig. S5).

From the pairwise mutation experiments, we conclude that at the AChR transmitter binding site (a) αW149 is energetically the most strongly linked residue; (b) the degree of coupling between side chains depends on the chemical nature of the substitutions; (c) the interactions, when present, are all unfavorable (reduce E_0 more than expected from independence); (d) αY93 in loop A has a different relationship with αW149 compared with the two loop C Tyr residues; and (e) the AChR gating isomerization is robust, insofar as receptors having all eight binding site aromatic residues in the two α subunits replaced with Arg still can isomerize between R and R* conformations.

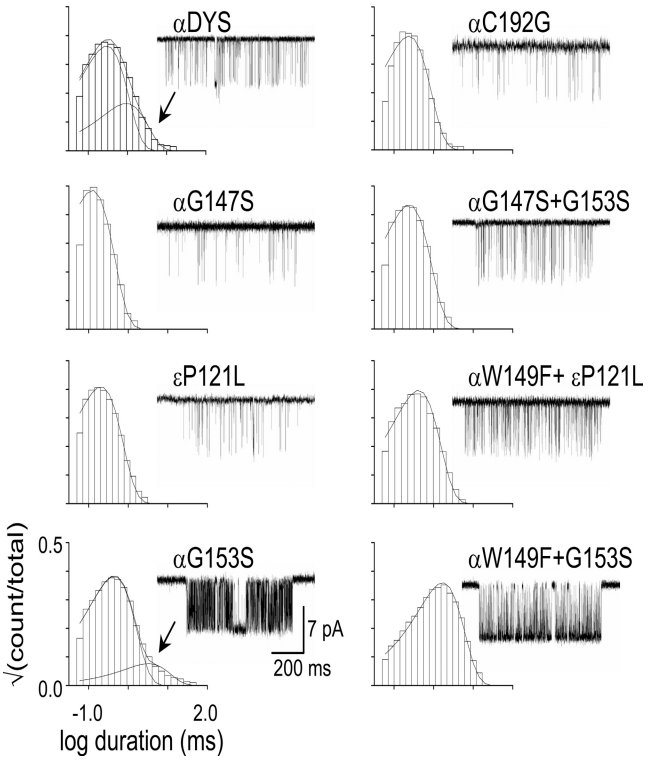

Figure 6. Mutations of nonaromatic binding site residues. Each panel shows an open-interval duration histogram and example cluster for the indicated mutation.

Mutations of nonaromatic residues

We also examined point mutations of four nonaromatic amino acids at the transmitter binding site (Fig. 6 and Table S5). Two Gly residues in loop B (αG147 and αG153) bracket αW149 (Fig. 2). The mutation αG147S produced a small (approximately eightfold) decrease in E_0, and the slow-channel congenital myasthenia mutation αG153S (Sine et al., 1995) produced a moderate (∼28-fold) increase in E_0. The mutation αC192G (at the tip of loop C) showed a small, approximately twofold reduction in E_0. The complementary binding site mutation εP121L, which was reported to reduce E_2 by ∼500-fold (Ohno et al., 1996), had no measurable effect on E_0. The mutations αC192G, αG147S, and εP121L eliminated the long component of spontaneous openings, but these were still apparent in the loop B mutant αG153S (Fig. 6).

We also made pairwise mutations involving some of these four positions (Table S5). The double mutant αG147S+αG153S reduced E_0 by 1.3-fold, which translates to a modest coupling energy of 0.9 kcal/mol. The other two combinations, αG153S+αW149F and εP121L+αW149F, showed little energetic coupling (−0.6 kcal/mol and 0.3 kcal/mol, respectively).

Multiple open components

The long open-interval lifetime component was absent after 57 of 60 different α-subunit binding site mutations of residues in loops A (αY93), B (αG147 and αW149), and C (αY190, αC192, and αY198). The three exceptions were αG153S, αY190G, and αY198G. The long open component was also not apparent in εP121L but was present after mutation of the complementary ε/δW55/57 residues to Arg or Glu.

To explore the origin of long openings, we recorded spontaneous currents from AChRs having both an αW149 side chain substitution that by itself eliminates the long openings and a secondary mutation that by itself does not. When the secondary mutation was nearby (αG153S) or at the complementary side of the binding site (εW55R/E or δW57R/E), the long open component vanished. When the additional mutation was at a distant position between the binding site and the gate (αP272A [the M2–M3 linker; Jha et al., 2007], αS269I [M2-28′; Mitra et al., 2005], δV269L [M2-13′; Cymes et al., 2002], δL265I/T [M2-9′; Cymes et al., 2002]), the long component vanished (Fig. 7 B). As shown in Fig. 7, mutation of the loop B residue αW149 eliminated long openings on all 10 backgrounds on which it was examined. This pattern suggests that spontaneous and brief versus long-duration open intervals reflect a structural fluctuation of the apo-protein that requires a Trp side chain at position α149. The structural elements that generate this spontaneous fluctuation include the protein, water, and extracellular ions (which are competitive inhibitors of the AChR transmitter binding site; Akk and Auerbach, 1996), perhaps in combination.

Published April , 2010

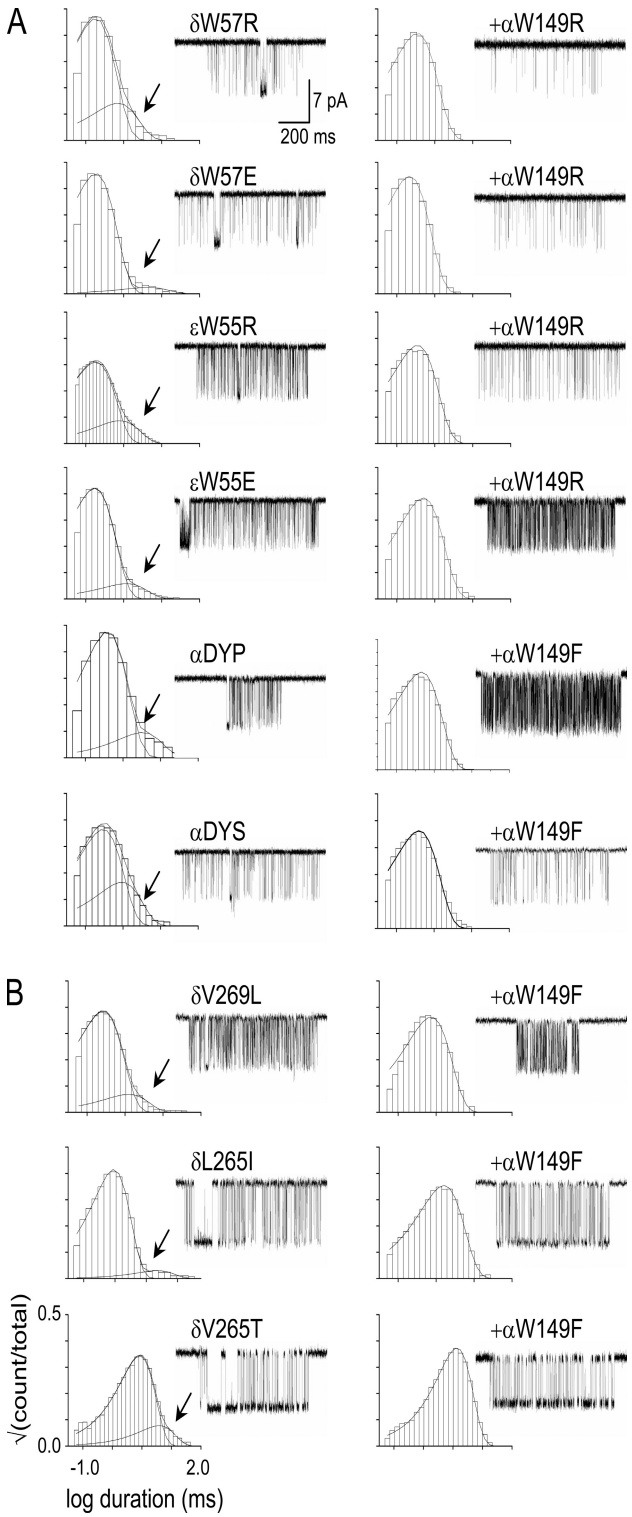

Figure 7. Mutations of αW149 yield one-component open-interval duration histograms on nine different background constructs. All panels show an example histogram (arrows, long components) and cluster. (left) Background mutation alone. (right) With an αW149 mutation. (A) α-Subunit extracellular domain background mutations (DYP is αD97A+αY127F+αP272A; DYS is αD97A+αY127F+αS269I). (B) δ-Subunit transmembrane domain (M2 helix) background mutations. In all cases, the αW149 mutation eliminates the long open component (Fig 6, bottom).

DISCUSSION

Fig. 2 C shows a close-up of the salient binding site residues in the 4-Å *Torpedo* AChR structure that possibly reflects an apo-R conformation (Unwin, 2005). There are no available AChR structures for liganded R or either liganded or apo-R*. However, there are structures of the homologous ACh-binding protein (AChBP), with and without bound ligands (Fig. 2 D; Brejc et al., 2001; Celie et al., 2004). AChBP has an affinity for ACh that is approximately midway (on a log scale) between that of R and R* in the AChR (Smit et al., 2001). Although this protein does not isomerize, a modified version of AChBP attached to the transmembrane domain of a 5-HT_{3A} receptor has been reported to generate currents when exposed to ACh (Bouzat et al., 2004). There is some indication that AChBP resembles the liganded R* conformation of AChRs (Brejc et al., 2001; Celie et al., 2004; Stewart et al., 2006).

We observe that in apo-AChRs, the binding site Trp residues (αW149 and εW55/δW57) experience significant energy changes in R↔R* gating. The range energy change caused by mutation of either of these positions is substantially larger than that caused by mutation of each of the three Tyr residues. On a per-residue basis, the energy change of the two Trp residues is about twice that of the three Tyr residues. In unliganded gating, the repositioning of the two Trp residues is an energetically significant event that occurs at the onset of the channel-opening process. The three Tyr residues show smaller positional changes between apo-AChR and apo-AChBP compared with the two Trp residues, which may move from being separated into an edge to face alignment (Samanta et al., 1999; Guvench and Brooks, 2005; Mahalakshmi et al., 2005).

The binding site aromatic residues appear to act as a coherent unit in the gating conformational change, with αW149 being an important main organizing element (Fig. 5 and Tables S3 and S4). With R substitutions, the energy changes at αW149 are coupled with those of the three Tyr residues and the complementary Trp residue. The three Tyr residues interact more strongly with αW149 than with each other or the complementary Trp. Also, the observation that the agonists αW149, αY93, and αY190 experience their gating changes at approximately the same point along the reaction coordinate suggests that these entities move in a concerted manner between their R and R* positions. αY198 has a lower Φ value, but we do not understand the significance of this observation.

We are unable to identify the chemical forces that correlate with these changes in residue energy. In particular, the results presented here pertain to unliganded AChRs; that is, with water molecules and perhaps ions occupying the space that is occupied by agonists in diliganded gating. Certainly, the presence of ACh would be

Published April , 2010

expected to significantly alter some aspects of the energy changes that we have measured. For example, the cation–π interaction that is present between αW149 and ACh (Gao et al., 1993; Zhong et al., 1998) would disappear in the apo-binding sites, and therefore we detect no preference of the R* conformation for aromatic substitutions at any of the positions we have probed. However, the fact that the Trp residues of AChBP are in the edge to face alignment at both liganded and apo-structures (Fig. 2 D) supports the hypothesis that the general shape of the R* transmitter binding site may be similar with and without bound agonists.

We can calculate the binding energy change experience by ligands from the relationship $K_d/J_d = \sqrt{(E_2/E_0)}$. There are published estimates of E_2 for AChR constructs (activated by ACh) having a Phe substitution at each aromatic position of the binding site (Chen et al., 1995; Akk et al., 1996, 1999; Akk, 2001, 2002; Bafna et al., 2009). As shown in Fig. 8 (also see Table S6), relative to the wt, the effect of a Phe substitution on the net binding energy (per site) was approximately threefold larger for positions αY190 and αW149 (∼1.8 kcal/mol) compared with positions αY93, αY198, and δ/εW55/57 (∼0.6 kcal/mol). The binding energy that drives gating appears to be derived mainly from interactions of ACh with αW149 and αY190.

We now analyze in detail the consequences of one of these binding site mutations. The published E_2^{ACh} value for αY190F is 0.035. For this mutant, $E_0 = 3.8 \times 10^{-7}$, so we calculate K_d/J_d = ∼303 (∼22 times lower than the wt). This single-atom perturbation reduces the per-site energy available for gating by ACh by 1.9 kcal/mol (from −5.2 to −3.3 kcal/mol). The published K_d^{ACh} value for αY190F is 5.2 mM, so we calculate J_d = ∼17 μM. Relative to the wt, the αY190F mutant shows an ∼800-fold reduction in E_2 that can be traced to an ∼1.7-fold reduction in E_0, an ∼35-fold increase in K_d, and an 80-fold increase in J_d.

Our results suggest that the structural perturbation that gives rise to spontaneous, long-lived openings occurs at the transmitter binding site. This event probably involves αW149 as well as other residues in all three binding site loops. Distant mutations did not affect the role of αW149 in this regard, which suggests that the salient binding site perturbation is a localized event. Although more experiments are needed to further identify the physical basis of the long open component, our results do not support the hypothesis that brief versus long spontaneous openings reflect AChRs having one versus two C loops in a capped position (Mukhtasimova et al., 2009).

The pattern of the energy change at the unliganded AChR transmitter binding sites suggests that early and energetically significant events in the channel-opening cascade derive from conformational changes of the two Trp residues. Analyses of Phe mutations of the binding site aromatics suggest that αY190 (loop C) and αW149 (loop B) provide the bulk of the net R* versus R ACh-binding energy. We hypothesize that the movements of these two residues are early events in the channel-opening conformational cascade. The unusual coupling of αW149 (loop B) with αY93 (loop A) is noteworthy.

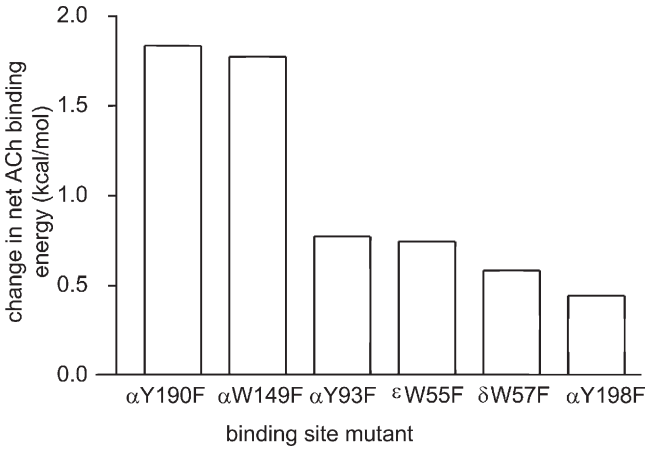

Figure 8. Effect of Phe substitutions on R versus R* ACh binding energy. The y axis is the net change in the R versus R* ACh binding free energy (= 0.59 ln $[(K_d/J_d)^{mut}/(K_d/J_d)^{wt}]$; Table S5). The mutations αY190F and αW149F cause the biggest drop in the net binding energy.

The E_0 estimates for many different constructs open the possibility of engineering the AChR transmitter binding site. These values, along with E_2 estimates, make it possible to calculate agonist-binding energy changes associated with gating and, thus, to identify the atomic forces between ligand, water, ions, and protein that promote the isomerization.

We thank M. Shero, M. Merritt, and M. Teeling for technical assistance. A. Auerbach wrote the manuscript; P. Purohit designed the experiments with A. Auerbach and analyzed all the data.

This work was supported by National Institutes of Health grant NS-064969.

Lawrence G. Palmer served as editor.

Submitted: 15 December 2009
Accepted: 9 March 2010

REFERENCES

Akk, G. 2001. Aromatics at the murine nicotinic receptor agonist binding site: mutational analysis of the alphaY93 and alphaW149 residues. *J. Physiol.* 535:729–740. doi:10.1111/j.1469-7793.2001.00729.x

Akk, G. 2002. Contributions of the non-alpha subunit residues (loop D) to agonist binding and channel gating in the muscle nicotinic acetylcholine receptor. *J. Physiol.* 544:695–705. doi:10.1113/jphysiol.2002.029413

Akk, G., and A. Auerbach. 1996. Inorganic, monovalent cations compete with agonists for the transmitter binding site of nicotinic acetylcholine receptors. *Biophys. J.* 70:2652–2658. doi:10.1016/S0006-3495(96)79834-X

Akk, G., S. Sine, and A. Auerbach. 1996. Binding sites contribute unequally to the gating of mouse nicotinic α D200N acetylcholine receptors. *J. Physiol.* 496:185–196.

Akk, G., M. Zhou, and A. Auerbach. 1999. A mutational analysis of the acetylcholine receptor channel transmitter binding site. *Biophys. J.* 76:207–218. doi:10.1016/S0006-3495(99)77190-0

Auerbach, A. 2005. Gating of acetylcholine receptor channels: brownian motion across a broad transition state. *Proc. Natl. Acad. Sci. USA.* 102:1408–1412. doi:10.1073/pnas.0406787102

Auerbach, A. 2010. The gating isomerization of neuromuscular acetylcholine receptors. *J. Physiol.* 588:573–586. doi:10.1113/jphysiol.2009.182774

Aylwin, M.L., and M.M. White. 1994. Ligand-receptor interactions in the nicotinic acetylcholine receptor probed using multiple substitutions at conserved tyrosines on the alpha subunit. *FEBS Lett.* 349:99–103. doi:10.1016/0014-5793(94)00649-0

Bafna, P.A., A. Jha, and A. Auerbach. 2009. Aromatic residues εTrp-55 and δTrp-57 and the activation of acetylcholine receptor channels. *J. Biol. Chem.* 284:8582–8588. doi:10.1074/jbc.M807152200

Bouzat, C., F. Gumilar, G. Spitzmaul, H.-L. Wang, D. Rayes, S.B. Hansen, P. Taylor, and S.M. Sine. 2004. Coupling of agonist binding to channel gating in an ACh-binding protein linked to an ion channel. *Nature.* 430:896–900. doi:10.1038/nature02753

Brejc, K., W.J. van Dijk, R.V. Klaassen, M. Schuurmans, J. van Der Oost, A.B. Smit, and T.K. Sixma. 2001. Crystal structure of an ACh-binding protein reveals the ligand-binding domain of nicotinic receptors. *Nature.* 411:269–276. doi:10.1038/35077011

Celie, P.H., S.E. van Rossum-Fikkert, W.J. van Dijk, K. Brejc, A.B. Smit, and T.K. Sixma. 2004. Nicotine and carbamylcholine binding to nicotinic acetylcholine receptors as studied in AChBP crystal structures. *Neuron.* 41:907–914. doi:10.1016/S0896-6273(04)00115-1

Chakrapani, S., T.D. Bailey, and A. Auerbach. 2003. The role of loop 5 in acetylcholine receptor channel gating. *J. Gen. Physiol.* 122:521–539. doi:10.1085/jgp.200308885

Chen, J., Y. Zhang, G. Akk, S. Sine, and A. Auerbach. 1995. Activation kinetics of recombinant mouse nicotinic acetylcholine receptors: mutations of alpha-subunit tyrosine 190 affect both binding and gating. *Biophys. J.* 69:849–859. doi:10.1016/S0006-3495(95)79959-3

Chiara, D.C., R.E. Middleton, and J.B. Cohen. 1998. Identification of tryptophan 55 as the primary site of [3H]nicotine photoincorporation in the gamma-subunit of the Torpedo nicotinic acetylcholine receptor. *FEBS Lett.* 423:223–226. doi:10.1016/S0014-5793(98)00093-3

Cymes, G.D., C. Grosman, and A. Auerbach. 2002. Structure of the transition state of gating in the acetylcholine receptor channel pore: a phi-value analysis. *Biochemistry.* 41:5548–5555. doi:10.1021/bi011864f

Edelstein, S.J., and J.-P. Changeux. 1998. Allosteric transitions of the acetylcholine receptor. *Adv. Protein Chem.* 51:121–184. doi:10.1016/S0065-3233(08)60652-X

Gao, J., L.W. Chou, and A. Auerbach. 1993. The nature of cation-π binding: interactions between tetramethylammonium ion and benzene in aqueous solution. *Biophys. J.* 65:43–47. doi:10.1016/S0006-3495(93)81031-2

Grosman, C. 2003. Free-energy landscapes of ion-channel gating are malleable: changes in the number of bound ligands are accompanied by changes in the location of the transition state in acetylcholine-receptor channels. *Biochemistry.* 42:14977–14987. doi:10.1021/bi0354334

Grosman, C., and A. Auerbach. 2000. Asymmetric and independent contribution of the second transmembrane segment 12′ residues to diliganded gating of acetylcholine receptor channels: a single-channel study with choline as the agonist. *J. Gen. Physiol.* 115:637–651. doi:10.1085/jgp.115.5.637

Grosman, C., M. Zhou, and A. Auerbach. 2000. Mapping the conformational wave of acetylcholine receptor channel gating. *Nature.* 403:773–776. doi:10.1038/35001586

Guvench, O., and C.L. Brooks III. 2005. Tryptophan side chain electrostatic interactions determine edge-to-face vs parallel-displaced tryptophan side chain geometries in the designed beta-hairpin "trpzip2". *J. Am. Chem. Soc.* 127:4668–4674. doi:10.1021/ja043492e

Hamill, O.P., A. Marty, E. Neher, B. Sakmann, and F.J. Sigworth. 1981. Improved patch-clamp techniques for high-resolution current recording from cells and cell-free membrane patches. *Pflugers Arch.* 391:85–100. doi:10.1007/BF00656997

Horovitz, A., and A.R. Fersht. 1990. Strategy for analysing the cooperativity of intramolecular interactions in peptides and proteins. *J. Mol. Biol.* 214:613–617. doi:10.1016/0022-2836(90)90275-Q

Jackson, M.B. 1984. Spontaneous openings of the acetylcholine receptor channel. *Proc. Natl. Acad. Sci. USA.* 81:3901–3904. doi:10.1073/pnas.81.12.3901

Jackson, M.B. 1986. Kinetics of unliganded acetylcholine receptor channel gating. *Biophys. J.* 49:663–672. doi:10.1016/S0006-3495(86)83693-1

Jha, A., and A. Auerbach. 2010. Acetylcholine receptor channels activated by a single transmitter molecule. *Biophys. J.* In press.

Jha, A., D.J. Cadugan, P. Purohit, and A. Auerbach. 2007. Acetylcholine receptor gating at extracellular transmembrane domain interface: the cys-loop and M2-M3 linker. *J. Gen. Physiol.* 130:547–558. doi:10.1085/jgp.200709856

Jha, A., P. Purohit, and A. Auerbach. 2009. Energy and structure of the M2 helix in acetylcholine receptor-channel gating. *Biophys. J.* 96:4075–4084. doi:10.1016/j.bpj.2009.02.030

Karlin, A. 2002. Emerging structure of the nicotinic acetylcholine receptors. *Nat. Rev. Neurosci.* 3:102–114. doi:10.1038/nrn731

Lester, H.A., M.I. Dibas, D.S. Dahan, J.F. Leite, and D.A. Dougherty. 2004. Cys-loop receptors: new twists and turns. *Trends Neurosci.* 27:329–336. doi:10.1016/j.tins.2004.04.002

Mahalakshmi, R., A. Sengupta, S. Raghothama, N. Shamala, and P. Balaram. 2005. Tryptophan-containing peptide helices: interactions involving the indole side chain. *J. Pept. Res.* 66:277–296. doi:10.1111/j.1399-3011.2005.00301.x

Mitra, A., G.D. Cymes, and A. Auerbach. 2005. Dynamics of the acetylcholine receptor pore at the gating transition state. *Proc. Natl. Acad. Sci. USA.* 102:15069–15074. doi:10.1073/pnas.0505090102

Mukhtasimova, N., W.Y. Lee, H.L. Wang, and S.M. Sine. 2009. Detection and trapping of intermediate states priming nicotinic receptor channel opening. *Nature.* 459:451–454. doi:10.1038/nature07923

Ohno, K., H.-L. Wang, M. Milone, N. Bren, J.M. Brengman, S. Nakano, P. Quiram, J.N. Pruitt, S.M. Sine, and A.G. Engel. 1996. Congenital myasthenic syndrome caused by decreased agonist binding affinity due to a mutation in the acetylcholine receptor epsilon subunit. *Neuron.* 17:157–170. doi:10.1016/S0896-6273(00)80289-5

O'Leary, M.E., G.N. Filatov, and M.M. White. 1994. Characterization of d-tubocurarine binding site of Torpedo acetylcholine receptor. *Am. J. Physiol.* 266:C648–C653.

Purohit, P., and A. Auerbach. 2007. Acetylcholine receptor gating: movement in the α-subunit extracellular domain. *J. Gen. Physiol.* 130:569–579. doi:10.1085/jgp.200709858

Purohit, P., and A. Auerbach. 2009. Unliganded gating of acetylcholine receptor channels. *Proc. Natl. Acad. Sci. USA.* 106:115–120. doi:10.1073/pnas.0809272106

Qin, F. 2004. Restoration of single-channel currents using the segmental k-means method based on hidden Markov modeling. *Biophys. J.* 86:1488–1501. doi:10.1016/S0006-3495(04)74217-4

Qin, F., A. Auerbach, and F. Sachs. 1997. Maximum likelihood estimation of aggregated Markov processes. *Proc. Biol. Sci.* 264:375–383. doi:10.1098/rspb.1997.0054

Samanta, U., D. Pal, and P. Chakrabarti. 1999. Packing of aromatic rings against tryptophan residues in proteins. *Acta Crystallogr. D Biol. Crystallogr.* 55:1421–1427. doi:10.1107/S090744499900726X

Sine, S.M., and A.G. Engel. 2006. Recent advances in Cys-loop receptor structure and function. *Nature.* 440:448–455. doi:10.1038/nature04708

Sine, S.M., P. Quiram, F. Papanikolaou, H.J. Kreienkamp, and P. Taylor. 1994. Conserved tyrosines in the alpha subunit of the nicotinic acetylcholine receptor stabilize quaternary ammonium groups of agonists and curariform antagonists. *J. Biol. Chem.* 269:8808–8816.

Sine, S.M., K. Ohno, C. Bouzat, A. Auerbach, M. Milone, J.N. Pruitt, and A.G. Engel. 1995. Mutation of the acetylcholine receptor alpha subunit causes a slow-channel myasthenic syndrome by enhancing agonist binding affinity. *Neuron.* 15:229–239. doi:10.1016/0896-6273(95)90080-2

Smit, A.B., N.I. Syed, D. Schaap, J. van Minnen, J. Klumperman, K.S. Kits, H. Lodder, R.C. van der Schors, R. van Elk, B. Sorgedrager, et al. 2001. A glia-derived acetylcholine-binding protein that modulates synaptic transmission. *Nature.* 411:261–268. doi:10.1038/35077000

Stewart, D.S., D.C. Chiara, and J.B. Cohen. 2006. Mapping the structural requirements for nicotinic acetylcholine receptor activation by using tethered alkyltrimethylammonium agonists and antagonists. *Biochemistry.* 45:10641–10653. doi:10.1021/bi060686t

Unwin, N. 2005. Refined structure of the nicotinic acetylcholine receptor at 4A resolution. *J. Mol. Biol.* 346:967–989. doi:10.1016/j.jmb.2004.12.031

Zhong, W., J.P. Gallivan, Y. Zhang, L. Li, H.A. Lester, and D.A. Dougherty. 1998. From ab initio quantum mechanics to molecular neurobiology: a cation-π binding site in the nicotinic receptor. *Proc. Natl. Acad. Sci. USA.* 95:12088–12093. doi:10.1073/pnas.95.21.12088

Zhou, Y., J.E. Pearson, and A. Auerbach. 2005. Φ-value analysis of a linear, sequential reaction mechanism: theory and application to ion channel gating. *Biophys. J.* 89:3680–3685. doi:10.1529/biophysj.105.067215